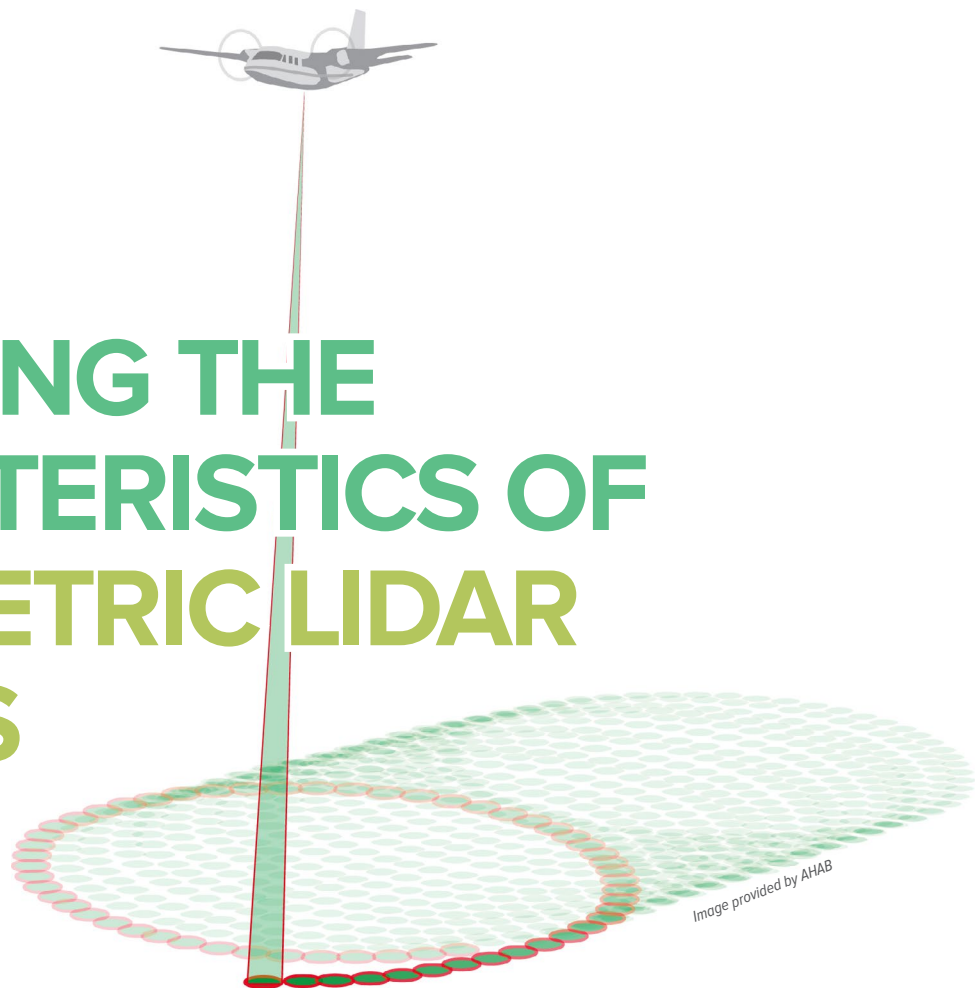


UNLOCKING THE CHARACTERISTICS OF BATHYMETRIC LIDAR SENSORS

Figure 1: Oblique elliptical scan pattern produced by Chiroptera and HawkEye III.



It's always tricky making detailed comparisons between different LiDAR sensors and technologies. Technical specifications often list different parameters, and even when they are the same, life is made more difficult by the use of different units.

For the first time we have a comparison table (see Table 1) listing the key specifications of the new bathymetric LiDAR sensors. The table goes some way to providing an insight into the nuances of each sensor, including

previously unlisted specifications, such as laser energy per pulse.

The table divides the sensors up into the traditional bathymetric LiDAR sensors, and topo-bathy sensors. The new topo-bathy LiDAR sensors bridge the divide between topographic and bathymetric LiDAR. The early EAARL sensor was the first of these beginning operations in 2001. Since then new sensors have been developed to efficiently measure both topographic and shallow bathymetric elevations.

It should be noted that all the LiDAR systems listed can measure both topographic data and bathymetry. The topographic data gathered from a traditional bathymetric LiDAR system tends to be of a lower density compared to that provided by a topo-bathy LiDAR sensor. The topo-bathy LiDAR sensors have a lower laser power, narrower beam, more frequent measurements and a smaller receiver field-of-view (FOV) (Dewberry 2012, Wright and Brock 2002). The HawkEye III system tends to cover both bases by having multiple lasers.

BY NATHAN D. QUADROS

One characteristic of interest are the *scan patterns* which are shown diagrammatically in the table. Some of the scanners are able to look forward and backward, increasing the number of times an area is sampled; although, this pattern does oversample the edges whilst under sampling the central part of the scan. This is demonstrated in **Figure 1** by the AHAB Chiroptera and HawkEye III sensors.

Figure 2 demonstrates an example where multiple looks are created by two bathymetric LiDAR systems installed in an aircraft. In this example Fugro LADS are able to fly the LADS Mk3 and Riegl VQ-820-G sensors in the same aircraft. The Riegl sensor is directed forward in this setup; however, it can also be configured to look backward.

Another interesting characteristic in the table is the *laser energy per pulse*. Although there are other factors involved, such as the receiver telescope area and FOV, the laser power combined with the pulse duration can be correlated to the depth penetration. The downside of higher laser energy per pulse is that the measurement frequency is generally lower than those systems with less energy per pulse. The main factor causing this is the limited energy per density dictated by the eye safety standard. The lower energy systems, like the Riegl VQ-820-G, have a much higher measurement frequency.

It is the *measurement frequency* which sets the topo-bathy LiDAR sensors apart from the traditional bathymetric LiDAR sensors. The high measurement frequency of topo-bathy sensors results in a closer point spacing, however, in order to obtain the high measurement frequency the depth penetration is sacrificed. It should be noted that higher measurement frequencies becomes more

superfluous as the depth increases. This is due to the unknown beam refraction. Therefore, the horizontal location and shape of each footprint is much less certain as a function of depth.

The *maximum water depths* listed by each manufacturer only tend to be reached in ideal conditions. The typical maximum water depths achieved in Australia and the Pacific tend to be reduced, mainly dependent upon the turbidity and seafloor bottom type. A general comparison in the table is provided against the Secchi depth; the Secchi depth being a simple ground-based measurement of water clarity.

One characteristic which is difficult to measure is the LiDAR *footprint diameter* due to the laser beam lacking a sharp edge. The $1/e^2$ width is used in this instance to define the nominal LiDAR footprint diameter. This measurement is the distance across the footprint between points which have an intensity equal to 13.5% of the maximum intensity within the footprint (Paschotta 2013). The sensors with higher laser energy per pulse tend to have a larger footprint.

In summary, it would be perilous to rate the various LiDAR sensors as better or worse, as each is unique in terms of bathymetry quality and cost. It is important to realise that all the sensors have unique capabilities, including those characteristics not listed in the table, such as receiver aperture area, and their individual capabilities i.e. HawkEye's ability to divide its receiver into multiple sections effectively reduces its footprint size; CZMIL's ability to divide its backscatter into seven small FOV segments and one large for deep water; and EAARL-B transmitting three beams and receiving them in three small FOV beams and one large one for deeper water.

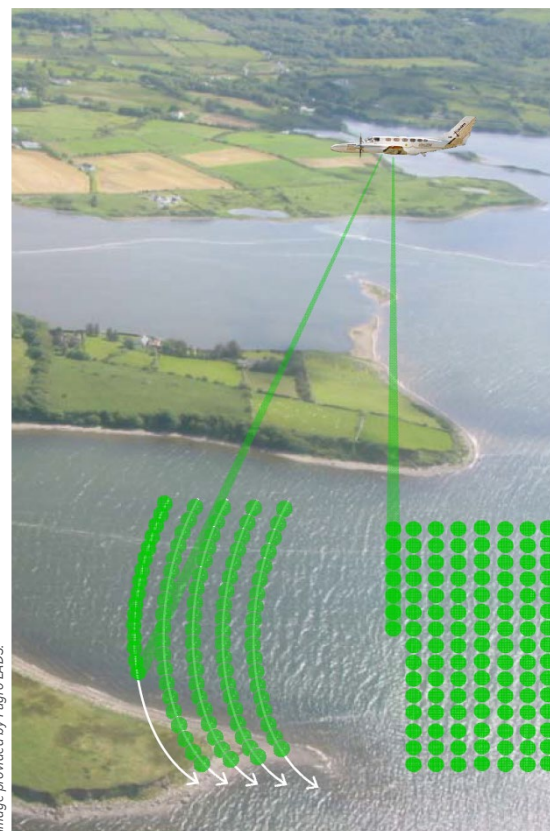



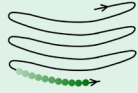
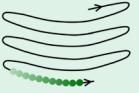
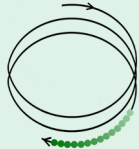
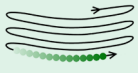
Image provided by Fugro LADS.

Figure 2: Diagram of airborne bathymetric LiDAR measuring the seafloor using both the Fugro LADS Mk3 and Riegl VQ-820-G operated by Fugro LADS.

It is the complete sensor package which provides the advantages and disadvantages. A decision of which sensor to use will be dependent upon the survey area, environment, project requirements and sensor availability. The most common aspects which tend to affect the choice of sensor relate to the maximum and minimum depths that need to be achieved, the level of detail inside the survey, and the products to be derived from the LiDAR data.

It is hoped that by providing an overview of the main characteristics of each LiDAR sensor, you will be in a more informed position at the start of your next bathymetry project.

Table 1: Bathymetric LiDAR Sensor Specifications

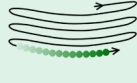
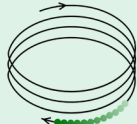
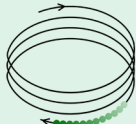
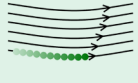
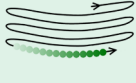
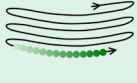
	Fugro LADS Mk3	Optech SHOALS 3000	Optech SHOALS 1000T	Optech CZMIL	Optech ALTM Aquarius
Typical Sensor Environment	Bathy	Bathy	Bathy	Topo-Bathy	Topo-Bathy
Origin	Australia	Canada	Canada	Canada	Canada
Year Released	2011	2010	2005	2011	2011
Still in Production	Yes	No	No	Yes	Yes
Laser Wavelength/s	Green 532nm	Green 532nm Infra-Red 1064nm	Green 532nm Infra-Red 1064nm	Green 532nm Infra-Red 1064nm	Green 532nm
Scan Pattern Diagram (Not to Scale)					
Scan Shape	Rectilinear	Circular Arc	Circular Arc	Circular	Elliptic Arc
Scan Direction and Angle From Nadir	Fwd up to 8°	Fwd 22°	Fwd 20°	Fwd and Aft 20°	Fwd 7°
Scan Method	Oscillating Mirror	Oscillating Mirror	Oscillating Mirror	Rotating Prisms	Oscillating Mirror
Laser Energy Per Pulse (Green 532nm)	7mJ	4mJ	4mJ	3mJ	0.1mJ
Pulse Duration	6.5ns	5ns	5ns	2.0–2.2ns	7ns
Peak Measurement Frequency	1.5kHz@532	3kHz@532	1kHz@532	10kHz@532 70kHz@1064	33–70kHz@532
532nm Nominal Footprint Diameter @ Water Surface (1/e ²)	3m	2m	2m	2.4m	0.3–0.6m @ AGL Below
Nominal Flying Height	400–915m AGL	300–400m AGL	300–400m AGL	400–800m AGL	300–600m AGL
Swath Width (as a function of point spacing or altitude)	585m@8x5m 360m@5x5m 125m@2.5x2.5m	160m@2x2m 300m@3x3m	60m@2x2m 130m@3x3m	291m@400m AGL 582m@800m AGL	up to 0.93 x AGL
Typical Bathymetric Point Spacings	2x2m–8x5m	2x2m–5x5m	2x2m–5x5m	2x2m (Deep) 0.7x0.7m (Shallow)	0.4x0.4m–1x1m
Maximum Depth	~80m 2.5–3 x Secchi depth	~50m 2–2.5 x Secchi depth	~50m 2–2.5 x Secchi depth	~60m 2.5–3 x Secchi depth	~20m 1 x Secchi depth
Minimum Depth	The minimum water depth of most systems has improved substantially in recent years.				
Vertical Accuracy	All LiDAR systems have the capability to meet the required IHO accuracy standards.				

Acknowledgements

The author wishes to thank Hugh Parker and Mark Penley *Fugro LADS*, David Collison and Joong Yong Park *Optech Inc*, Swante Welander *Airborne Hydrography*

(*AHAB*), Martin Pfennigbauer *Riegl*, and John Brock and Charles W Wright the *U.S. Geological Survey (USGS)* for their contribution and providing the specifications of their LiDAR sensors. ■

Dr Nathan Quadros completed his Ph.D. in 2008 investigating issues with airborne LiDAR in the coastal zone. He is currently delivering bathymetric and topographic LiDAR to Tonga, PNG, Vanuatu and Samoa, along with the training and capacity building for these country governments to use the data.

AHAB HawkEye IIB	AHAB HawkEye III	AHAB Chiroptera	Riegl VQ-820-G	USGS EAARL-B	NASA EAARL
Bathy	Bathy/Topo-Bathy	Topo-Bathy	Topo-Bathy	Topo-Bathy	Topo-Bathy
Sweden	Sweden	Sweden	Austria	USA	USA
2009	2013	2012	2011	2012	2001
No	Yes	Yes	Yes	Yes	No
Green 532nm Infra-Red 1064nm	Green 532nm x 2 (Deep and Shallow) Infra-Red 1064nm	Green 532nm Infra-Red 1064nm	Green 532nm	Green 532nm	Green 532nm
					
Elliptic Arc	Elliptical	Elliptical	Elliptic Arc	Elliptic Arc	Elliptic Arc
Fwd 20°	Fwd and Aft 14° Sideways 20°	Fwd and Aft 14° Sideways 20°	Fwd or Aft 20°	Fwd 5° Sideways 22°	Fwd 5° Sideways 22°
Oscillating Mirror	Palmer Scanner	Palmer Scanner	Rotating Multi-Facet Mirror	Oscillating Raster Scanner	Oscillating Raster Scanner
3mJ	3mJ Deep (D) 0.1mJ Shallow (S)	0.1 mJ	0.02mJ	0.4mJ 0.13mJ per beam	0.08mJ
4ns	4ns (D) 2.5ns (S)	4ns	1.2ns	0.85ns	1.2ns
4kHz@532 128kHz@1064	10kHz@532 (D) 35kHz@532 (S) 400kHz@1064	36kHz@532 400kHz@1064	Up to 512kHz@532	15kHz or 30kHz	5kHz
6m	3m (D) 1.5m (S)	1.5m	0.6m @ AGL Below	0.3m per beamlet, 1.6m apart	0.2m
250–500m AGL	400–1000m AGL	250–600m AGL	Nominal 600m AGL	Nominal 300m AGL	300–400m AGL
160m–260m @400m AGL 100m@250m AGL	290m@400m AGL 730m@1000m AGL	300m @400m AGL	400m	230m @300m AGL	230m @300m AGL
0.5x0.5m– 3.5x3.5m	1.7x1.7–3.3x3.3m (D) 0.4x0.4–0.8x0.8m (S)	0.4x0.4m–1 x 1m	0.2x0.2m–0.8x0.8m	1.5 x 1.5m	2 x 3m
~50m 2–3 x Secchi depth	~50m 2–3 x Secchi depth	~20m 1 x Secchi depth	~10m 1 x Secchi depth	~27m 1.5–2.5 x Secchi depth	~27m 1.5–2.5 x Secchi depth

The minimum depth is now less than 0.2m for most sensors.

Vertical accuracy is dependent on survey design and processing.

References

- Dewberry 2012. *Final Report of the National Enhanced Elevation Assessment*. United States Geological Service. pp. 817
- Paschotta, R. 2013. *RP Photonics Encyclopaedia*. http://www.rp-photonics.com/beam_radius.html. Accessed 04/10/2013.
- Wright C.W. and Brock J.C. 2002 *EAARL: A LiDAR for Mapping Shallow Coral Reefs and Other Coastal Environments*. Proceedings of the Seventh International Conference on Remote Sensing for Marine and Coastal Environments, 20-22
- Quadros, Nathan: Research reports available online at <http://www.crcsi.com.au/Research/Commissioned-Research/UDEM-for-CC>.